Small Angle X-Ray Scattering Studies and Modeling of *Eudistylia vancouverii* Chlorocruorin and *Macrobdella decora* Hemoglobin

Angelika Krebs,* Helmut Durchschlag,† and Peter Zipper‡
*Structural and Computational Biology Programme, European Molecular Biology Laboratory, Heidelberg, Germany; †Institute of Biophysics and Physical Biochemistry, University of Regensburg, Germany; and ‡Physical Chemistry, Institute of Chemistry, University of Graz, Austria

ABSTRACT Annelids possess giant extracellular oxygen carriers that exhibit a hexagonal bilayer appearance and have molecular masses of ~3.5 MDa. By small angle x-ray scattering (SAXS), *Eudistylia vancouverii* chlorocruorin and *Macrobdella decora* hemoglobin were investigated in solution. On the basis of the experimental SAXS data, three-dimensional models were established in a two-step approach (trial and error and averaging). The main differences between the complexes concern the structure of their central part and the subunit architecture. Usage of our SAXS models as templates for automated model generation (program DAMMIN) led to refined models that fit perfectly the experimental data. Special attention was paid to the inhomogeneous density distribution observed within the complexes. DAMMIN models without a priori information could not reproducibly locate low-density areas. The usage of templates, however, improved the results considerably, in particular by applying electron microscopy-based templates. Biologically relevant information on the presence of low-density areas and hints for their presumable location could be drawn from SAXS and sophisticated modeling approaches. Provided that different models are analyzed carefully, this obviously opens a way to gain additional biologically relevant structural information from SAXS data.

INTRODUCTION

Extracellular annelid hemoglobins are giant molecules that have a characteristic two-tiered hexagonal bilayer (HBL) appearance in electron micrographs; they exhibit high cooperativity of oxygen binding and low iron and heme contents (Vinogradov et al., 1982; Kapp et al., 1990; Qabar et al., 1991; Lamy et al., 1996; for a recent review, see Weber and Vinogradov, 2001). The hemoglobin of the earthworm *Lumbricus terrestris* (*Lumbricus* Hb) is the most extensively studied annelid hemoglobin. The complex has an overall D6 symmetry (Royer and Hendrickson, 1988; Boekema and van Heel, 1989). Due to considerable differences in the mass estimations, the exact stoichiometry of the components was unclear for a long time (Martin et al., 1996b; Zhu et al., 1996). Two models have been proposed to explain the architecture of *Lumbricus* Hb: The first model comprises 24 octameric subassemblies of globin chains and 24 linker chains (Ownby et al., 1993). In the second, the so-called ''bracelet model'' (Vinogradov et al., 1986, 1991; Martin et al., 1996a,b), 12 dodecameric 200-kDa subunits, each composed of three monomeric and three trimeric heme-containing globin chains, and 36 heme-deficient linker chains form the HBL complex with a total mass of ~3.5 MDa.

For *Lumbricus* Hb, several three-dimensional (3D) reconstructions from cryoelectron microscopy have been presented (Schatz et al., 1995; de Haas et al., 1997; Taveau et al., 1999; Mouche et al., 2001). Recently the crystal structure at 0.55 nm resolution was published (Royer et al., 2000), revealing an organization of 144 oxygen-binding hemoglobin subunits and 36 nonhemoglobin linker subunits, similar to the bracelet model. Thus, in the case of *Lumbricus* Hb, the picture of its structure has obtained a very detailed level over the years.

Less structural information is available for other related oxygen-carrying proteins. Bracelet architectures, similar to *Lumbricus* Hb, have been suggested for *Macrobdella decora* hemoglobin (*Macrobdella* Hb; de Haas et al., 1996a) and for *Eudistylia vancouverii* chlorocruorin (*Eudistylia* Chl; de Haas et al., 1996b), although the exact number of globin and linker chains is still unknown. These studies show subunits that appear somewhat hollow in the center (hollow globular substructures), similar to the subunits of *Lumbricus* Hb (Schatz et al., 1995; de Haas et al., 1997; Taveau et al., 1999; Mouche et al., 2001).

The investigation of the 3D structure of the giant annelid hemoglobins is essential for a better understanding of their complex architecture and functionality. In this context, small angle x-ray scattering (SAXS) is a potent tool for studying the solution structure of such giant proteins at low resolution (Kapp et al., 1990; Krebs et al., 1996, 1998). In this study, we used the SAXS technique to investigate *Eudistylia* Chl and *Macrobdella* Hb and to determine their radius of gyration, R_G, molar mass, M, maximal diameter, d_{max}, hydrated volume, V, and shape. The experimentally obtained data were simulated by 3D models consisting of a large number of small spheres. These SAXS models were constructed by trial and error in a two-step procedure leading to consensus models. In addition, SAXS models were also created by using the advanced modeling procedure

Submitted December 2, 2003, and accepted for publication April 12, 2004.

Address reprint requests to Dr. Angelika Krebs, Structural and Computational Biology Programme, European Molecular Biology Laboratory, Meyerhofstrasse 1, D-69117 Heidelberg, Germany. Tel.: 49-6221-387256; Fax: 49-6221-387306; E-mail: krebs@embl-heidelberg.de.

0006-3495/04/08/1173/13 $2.00

doi: 10.1529/biophysj.103.037929

implemented in the program DAMMIN (Svergun, 1999, 2000) in several alternatives (cf. Zipper et al., 2004). All models were compared on the basis of their fit with the experimental data; for a visual comparison they were displayed as surface-rendered densities. Furthermore, the models were used as bases for the prediction of hydrodynamic parameters.

MATERIALS AND METHODS

Eudistylia Chl and *Macrobdella* Hb, isolated as described previously (Vinogradov and Sharma, 1994), were provided by S. N. Vinogradov (Department of Biochemistry and Molecular Biology, Wayne State University, Detroit, MI). For SAXS experiments, highly concentrated solutions of the oxygenated proteins were dialyzed against 0.1 M Tris/HCl buffer, 1 mM EDTA, pH 7.0. A dilution with dialysis buffer led to final protein concentrations between 5 and 80 mg/ml.

SAXS experiments were carried out at 4°C by means of a Kratky compact camera (A. Paar, Graz, Austria), using copper radiation (wavelength $\lambda = 0.154$ nm) from a conventional x-ray tube, and a proportional counter. Scattering measurements were performed in the angular range of $2\theta = 0.7$–57 mrad, corresponding to h values of 0.029–2.3 nm^{-1} ($h = (4\pi/\lambda)\sin\theta$; θ is half the scattering angle). Both proteins were investigated under the same conditions, and the data were evaluated in the same way as reported previously for *Lumbricus* Hb (Krebs et al., 1996), to establish a founded basis for the comparison of the low-resolution structures of these HBL complexes.

All scattering curves were measured repeatedly. With each protein, two independent series of experiments were performed, each comprised measurements at four different concentrations between 5 and 15 mg/ml in the angular range below 7 mrad and measurements at high concentrations (67 or 80 mg/ml) over the full range mentioned above. A minimum of three scattering curves was recorded for each protein concentration in each series. The measured intensities were corrected for background scattering, and the low-concentration data were extrapolated to zero concentration before the necessary corrections for the beam geometry were applied. This desmearing procedure was performed by means of the program ITP (Glatter, 1977) and led to scattering curves, $I(h)$, and pair-distance distribution functions, $p(r)$ (Glatter and Kratky, 1982). The molecular parameters R_G and d_{max} were determined from the $p(r)$ functions, M from the absolute scattering intensity at zero angle, and V from Porod's invariant. To obtain representative patterns of the proteins, the scattering curves, $p(r)$ functions, and molecular parameters of each complex were averaged over the repeated measurements; only averaged data are discussed in the following. The calculated limits of error in Fig. 1 and Table 1 reflect the reproducibility of the data rather than their absolute accuracy.

A finite element method (representation of the molecular structure by an ensemble of small spheres: bead modeling) was used for the model calculations to simulate the experimental data. Exploiting the experimental SAXS curves of the proteins, consensus models were established by a two-step approach consisting of finding appropriate models by trial and error and subsequently averaging the best fits (cf. Krebs et al., 1998). Alternatively, models were generated by an advanced modeling approach (program DAMMIN; Svergun, 1999, 2000), an automated procedure based on simulated annealing, which uses compactness and connectivity constraints and, optionally, a priori structural information. To speed up the computations, the program uses spherical harmonics to calculate the model intensity. The input of experimental data occurs via a GNOM file (Semenyuk and Svergun, 1991). This modeling approach was applied either without a priori structural information (ab initio modeling) or by using templates derived from the original SAXS consensus models or from 3D electron microscopy (EM) reconstructions (de Haas et al., 1996a,b). The templates were produced by a similar procedure as described previously (Zipper et al., 2004). For generating templates from the 3D EM reconstructions, a rescaling step was performed to obtain the proper angular position of the first submaximum in the scattering curve of the basic EM model (cf. Krebs et al., 1998); an additional upscaling of the coordinates of the EM templates by a factor of 1.05 was applied in some cases to reduce the effects of DAMMIN's peripheral penalty.

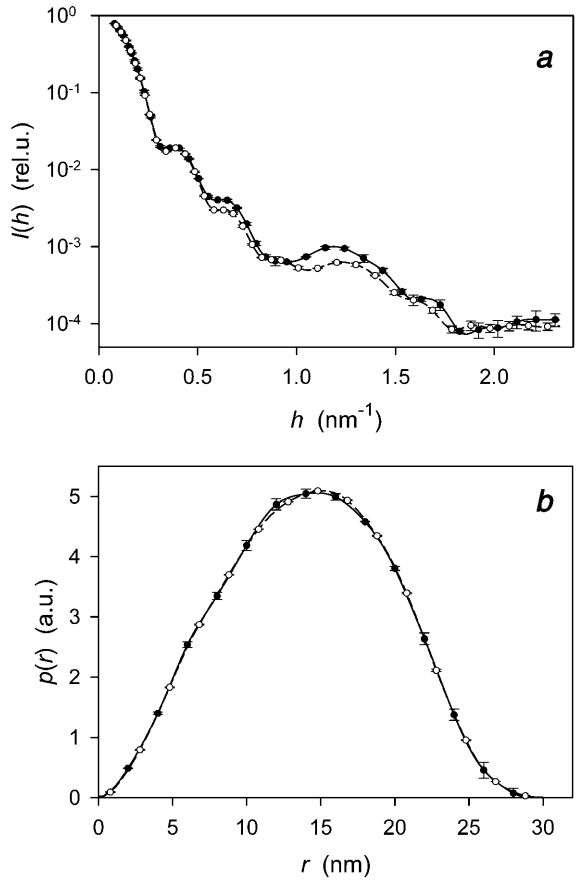

FIGURE 1 Experimental SAXS data from *Eudistylia* Chl (*solid lines* and *solid circles* with *error bars*) and *Macrobdella* Hb (*dashed lines* and *open circles* with *error bars*): (*a*) normalized desmeared scattering curves $I(h)$ and (*b*) pair-distance distribution functions $p(r)$. The symbols are only drawn for every fifth data point. The error bars represent the standard deviations resulting from averaging the data from repeated measurements.

Calculations of scattering curves and $p(r)$ functions from the coordinates of the spheres were performed with several programs based on Debye's formula and other algorithms outlined in Glatter (1980) and Glatter and Kratky (1982). For the trial-and-error models, the radius of the spheres was chosen so that a continuum was simulated by an appropriate overlap of the spheres. For the Debye calculation of scattering curves from the DAMMIN models, the size of the spheres was reduced to optimize the comparison with the curves provided directly by DAMMIN (Zipper et al., 2004). In general, the $p(r)$ functions of models were calculated by Fourier transformation of the scattering curves. Hydrodynamic parameters (sedimentation coefficient s and translational diffusion coefficient D) of the models were predicted by application of the program HYDRO (García de la Torre et al., 1994, 2000).

The program RASMOL (Sayle and Milner-White, 1995) was adopted for the primary graphical representation of all models obtained. Surface representations of the models were applied to allow a closer comparison of the structural features of the various protein models. For this purpose, electron density maps were generated from the coordinates of the spheres with programs from the CCP4 package (Collaborative Computational Project, Number 4, 1994). Threshold levels were chosen in a way that all

TABLE 1 Experimental SAXS parameters and data of trial-and-error SAXS models of annelid hemoglobins

Parameter	*Eudistylia* Chl		*Macrobdella* Hb		*Lumbricus* Hb	
	Exp.*†	Model‡	Exp.*†	Model‡	Exp.†§	Model‡
R_G (nm)	10.73 ± 0.09	10.64 ± 0.05	10.75 ± 0.01	10.73 ± 0.02	10.71 ± 0.02	10.68 ± 0.04
d_{max} (nm)	29.05 ± 0.07	29.2 ± 0.1	29.54 ± 0.02	29.6 ± 0.1	29.37 ± 0.21	29.6 ± 0.1
V (nm^3)	5100 ± 100	5300 ± 100	5800 ± 300	6000 ± 300	6200 ± 200	6200 ± 400
M (kg/mol)¶	3000 ± 300		3300 ± 200		3500 ± 200	
r_b (nm)		0.66		0.66		0.66
d_x (nm)‖		29.2 ± 0.1		29.2 ± 0.1		29.2 ± 0.1
d_y (nm)‖		27.2 ± 0.1		27.7 ± 0.8		27.3 ± 0.2
d_z (nm)‖		17.3 ± 0.1		19.4 ± 1.7		19.8 ± 1.9
Consensus model:						
Number of models included (N_m)		6		4		22
Total number of spheres (N_b)		4551		5970		6844
Number of spheres per subunit**		337		325		333
Number of spheres in the central unit**		89		36		83

*Experimental data are taken from Krebs (1996).
†Mean values and standard deviations result from averaging experimental data.
‡Mean values and standard deviations result from averaging individual models.
§Experimental data are taken from Krebs (1996) and Krebs et al. (1996, 1998).
¶The partial specific volume of $\bar{v} = 0.733$ cm^3/g found for *Lumbricus* Hb (Shlom and Vinogradov, 1973) was also used for calculating the molar masses of *Eudistylia* Chl and *Macrobdella* Hb.
‖The values for d_x, d_y and d_z refer to the largest dimension in each direction, obtained from the difference of sphere coordinates by adding the diameter of one sphere.
**Only high-weight spheres, occurring in at least N_m-1 models, are taken into account.

models represented the same volume. The electron densities were displayed by VOLVIS (Research Foundation of the State University of New York).

RESULTS

Experimental SAXS data and SAXS models

In Fig. 1, normalized scattering curves $I(h)$ and distance distribution functions $p(r)$ of *Eudistylia* Chl and *Macrobdella* Hb are shown. The scattering behavior of these proteins appears to be quite similar. The proteins obviously possess a highly symmetrical structure that gives rise to distinct maxima and minima in the scattering curves (cf. Glatter and Kratky, 1982); the differences in their intensities, however, suggest some differences in the protein architecture. Resulting SAXS parameters, e.g., R_G, d_{max}, V, and M, are listed in Table 1, together with the corresponding data for *Lumbricus* Hb (Krebs, 1996; Krebs et al., 1996, 1998). Our experimental values for R_G and d_{max} of *Macrobdella* Hb are compatible with those of 10.5 (±0.2) nm and 28.0 (±0.5) nm, respectively, found in previous SAXS studies (Kapp et al., 1990), whereas our value for V is considerably smaller than the volume of 7500 (±300) nm^3 reported earlier; our value for M is similar to that of 3500 (±300) kg/mol found previously (Schmuck, 1989). For *Eudistylia* Chl, SAXS reference data are not available in the literature.

SAXS models were built from identical spheres of radius $r_b = 0.66$ nm. Experimental values for R_G and d_{max} and the shapes of the $I(h)$ and $p(r)$ patterns were used as selection criteria for modeling based on an assumed HBL structure. For our models, a two-step approach turned out to be useful. In the first step, a number of different models were developed by trial and error. None of these models provided a perfect fit to the experimental scattering curve. In the second step, a consensus model was constructed by averaging the best-fitting models of the first step. Due to this averaging, the initially identical spheres were replaced with spheres of individual statistical weightings. These weightings were derived from the frequency of occupancy of given positions in the various models. The highest weighting was given to positions that were occupied in all models and the lowest to positions occupied only in a single model. By this procedure, the original two-level density distributions of the individual models (with a value of 1 corresponding to matter and 0 corresponding to void) were transformed into a multilevel density distribution reflecting different levels of probability of the positions in the resulting consensus model. In this context, it has to be noted that in the interior of the consensus model inhomogeneities in its density distribution can only occur if the distributions of the individual models themselves are inhomogeneous.

The resulting consensus models for *Eudistylia* Chl and *Macrobdella* Hb are shown in Fig. 2, *A* and *B*. The models of both complexes are composed of 12 identical subunits in an eclipsed HBL structure, and in the center of each model an additional central unit is assumed. The different weighting of the spheres is expressed by different shades of gray: dark is used for spheres with the highest weighting, and the light spheres indicate areas of less probability. Essential structural parameters are given in Tables 1 and 2, together with the corresponding data for *Lumbricus* Hb.

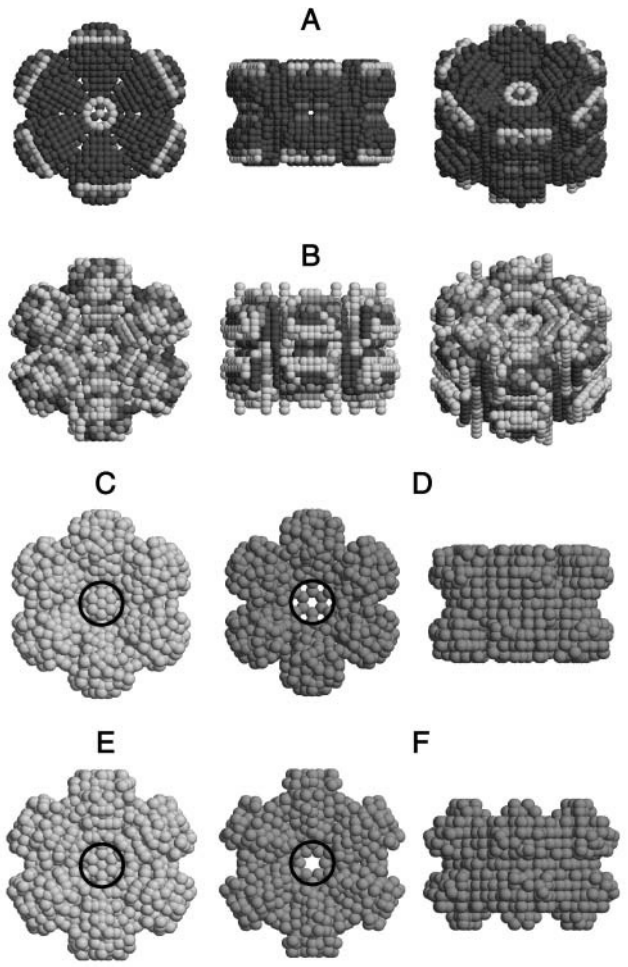

FIGURE 2 Different views of SAXS consensus models of *Eudistylia* Chl (*A*) and *Macrobdella* Hb (*B*) and of templates (*C* and *E*) and SAXS-biased DAMMIN models (*D* and *F*) derived therefrom. The consensus models were created by averaging the structures of several trial-and-error models each of which provided a good but not perfect fit to the experimental scattering curve of the protein under analysis. A continuous electron density was simulated by overlapping spheres arranged in a regular way. The consensus model of *Eudistylia* Chl (*A*) is based on six different models and that of *Macrobdella* Hb (*B*) is the result of averaging four models. The frequency of occurrence of the spheres in the underlying models, a measure of probability, is expressed by different shades of gray (*light*: low frequency, equivalent to low probability; *dark*: high frequency). The SAXS-biased DAMMIN models of *Eudistylia* Chl (*D*) and *Macrobdella* Hb (*F*) were obtained using templates that were derived from the consensus models. The templates (*C* and *E*) consist of beads with $r_b = 0.8$ nm, placed at local centers of gravity. Therefore the spheres are not arranged as regularly as in the original SAXS models and overlap considerably. Application of DAMMIN results in the simulation of less mass in the center of the models (see *black circles*). SAXS parameters of the proteins and models are listed in Tables 1 and 2, scattering curves and $p(r)$ functions of the models are shown in Fig. 4.

To improve the visualization of the models, density maps were created from the coordinates of the spheres and were presented in surface rendering. For this purpose the initially high number of spheres of the consensus models was reduced to be compatible with other models of this study. Fig. 3 *a* shows surface representations of the resulting density maps for *Eudistylia* Chl (*A–D*) and *Macrobdella* Hb (*E–H*). Both models possess a low density in the molecule center and little density in certain areas of the subunits. The *Macrobdella* Hb model simulates less density in the central unit than that of *Eudistylia* Chl, an aspect that is obvious from a comparison of the top views of the models (cf. *arrows*) and is also suggested by the different numbers of high-weight spheres in the central unit (Table 1).

Fig. 4 presents comparisons of model and experimental $I(h)$ and $p(r)$ patterns of *Eudistylia* Chl (*A* and *B*) and *Macrobdella* Hb (*C* and *D*). The scattering curves of the SAXS consensus models (*green lines*) agree fairly with the experimental profiles (*black lines*) in the angular range $h < 1.0$ nm^{-1} (Fig. 4, *A* and *C*). In this range, however, the second and third minimum of the scattering curve of *Eudistylia* Chl are not modeled satisfactorily (Fig. 4 *A*). The model of *Macrobdella* Hb fits the second minimum of the experimental $I(h)$ quite well, but the fit of the third minimum is insufficient (Fig. 4 *C*). In a similar way, the consensus models of both proteins do not fit the $p(r)$ functions perfectly (Fig. 4, *B* and *D*).

SAXS-biased DAMMIN models

In an attempt to improve the original SAXS consensus models, these were used as a priori information for the automated generation of models by DAMMIN (Svergun, 1999, 2000). For this purpose, appropriate templates were established from the consensus models according to the following procedure. First the selected model was superimposed in six rotation states. A subsequent data-reduction step (Zipper and Durchschlag, 2000) using a hexagonal lattice of definite cell size (1.6 nm) led to an intermediate template. Finally one-twelfth of the reduced structure was used to create the final template with exact D6 symmetry as required by DAMMIN (for a detailed description see Zipper et al., 2004).

In this procedure, the different weightings of the spheres of the consensus models were not considered, but all spheres were treated as identical. Thus the templates, defining the search space for the subsequent DAMMIN approach, were made up from the entire set of occupied positions in the SAXS models underlying the consensus models, without preferring any particular model configuration. When performing the data reduction step, the resulting spheres were

TABLE 2 Parameters of consensus and DAMMIN models of annelid hemoglobins

	Eudistylia Chl	*Macrobdella* Hb	*Lumbricus* Hb
SAXS consensus model			
R_x, R_y (nm)	6.84	6.90	6.82
R_z (nm)	4.45	4.47	4.60
d_z (nm)	17.3	21.6	21.5
D* (10^{-7} cm^2/s)	1.67	1.64	1.63
s* (10^{-13} s)	64.1	62.8	62.4
Mean values of SAXS-biased DAMMIN models			
Number of models	3	3	3
N_b†	1452 ± 34 1558	1616 ± 23 1818	1777 ± 4 1957
V‡ (nm^3)	5150 ± 120	5732 ± 80	6303 ± 15
R_G (nm)	10.78 ± 0.01	10.78 ± 0.01	10.71 ± 0.00
R_x, R_y (nm)	6.90 ± 0.02	6.92 ± 0.02	6.87 ± 0.01
R_z (nm)	4.56 ± 0.06	4.49 ± 0.06	4.49 ± 0.04
d_z (nm)	17.6 ± 0.0	19.4 ± 1.6	18.3 ± 1.2
D (10^{-7} cm^2/s)	1.61 ± 0.00	1.60 ± 0.01	1.61 ± 0.00
s (10^{-13} s)	61.9 ± 0.1	61.3 ± 0.4	61.9 ± 0.1
Mean values of ab initio DAMMIN models			
Number of models	11	11	27
N_b	1505 ± 17	1662 ± 44	1826 ± 44
V‡ (nm^3)	5337 ± 59	5895 ± 155	6477 ± 156
R_G (nm)	10.78 ± 0.02	10.79 ± 0.01	10.71 ± 0.01
R_x, R_y (nm)	6.95 ± 0.07	6.89 ± 0.06	6.87 ± 0.05
R_z (nm)	4.41 ± 0.23	4.61 ± 0.18	4.50 ± 0.14
d_z (nm)	20.1 ± 1.9	22.5 ± 2.2	20.4 ± 1.6
D (10^{-7} cm^2/s)	1.58 ± 0.03	1.55 ± 0.02	1.59 ± 0.02
s (10^{-13} s)	60.7 ± 1.0	59.8 ± 0.8	60.9 ± 0.9
Mean values of EM-biased DAMMIN models			
Beads on lattice points			
Number of models	8	8	8
N_b	1449 ± 19	1620 ± 31	1785 ± 43
V‡ (nm^3)	5138 ± 66	5746 ± 111	6331 ± 153
R_G (nm)	10.77 ± 0.01	10.78 ± 0.01	10.71 ± 0.01
R_x, R_y (nm)	6.91 ± 0.05	6.94 ± 0.03	6.84 ± 0.03
R_z (nm)	4.52 ± 0.14	4.45 ± 0.07	4.56 ± 0.07
d_z (nm)	17.6 ± 0.0	17.6 ± 0.0	17.6 ± 0.0
D (10^{-7} cm^2/s)	1.61 ± 0.01	1.61 ± 0.02	1.62 ± 0.01
s (10^{-13} s)	61.6 ± 0.5	61.9 ± 0.6	62.0 ± 0.3
Beads on centers of gravity			
Number of models	4	4	4
N_b	1786 ± 40	1701 ± 46	2132 ± 59
V§ (nm^3)	5140 ± 111	5745 ± 157	6330 ± 175
R_G (nm)	10.71 ± 0.01	10.76 ± 0.02	10.67 ± 0.03
R_x, R_y (nm)	6.93 ± 0.02	6.91 ± 0.02	6.83 ± 0.03
R_z (nm)	4.30 ± 0.02	4.48 ± 0.04	4.54 ± 0.03
d_z (nm)	17.3 ± 0.0	17.3 ± 0.1	18.5 ± 1.3
D (10^{-7} cm^2/s)	1.65 ± 0.00	1.65 ± 0.00	1.63 ± 0.01
s (10^{-13} s)	63.4 ± 0.1	63.5 ± 0.1	62.5 ± 0.2

Experimental SAXS parameters (R_G and V) of all hemoglobins under analysis are given in Table 1. Experimental hydrodynamic parameters (s and D) span a wide range of values for *Lumbricus* Hb: $s = 58.9$–61.1×10^{-13} s (e.g., Svedberg and Eriksson, 1933; Svedberg, 1937; Rossi Fanelli et al., 1970; Shlom and Vinogradov, 1973; David and Daniel, 1974; Gros, 1978) and $D = 1.3$–1.81×10^{-7} cm^2/s (e.g., Svedberg, 1937; Shlom and Vinogradov, 1973; Gros, 1978), with $(1.66 \pm 0.05) \times 10^{-7}$ cm^2/s (Shlom and Vinogradov, 1973) as a probable value for D; for *Eudistylia* Chl, only one value has been mentioned: $s = 56.5 \times 10^{-13}$ s (Terwilliger et al., 1975). DAMMIN models were calculated using $r_b = 0.8$ nm. R_x, R_y, and R_z are the axial radii of gyration of the corresponding model in the x, y, and z directions, respectively, and d_z symbolizes the largest dimension in the z direction. D values are calculated directly from the coordinates and radii of the spheres, whereas the quantities M and $\bar{v}$ are additionally required for predictions of s; in agreement with previous studies (Zipper et al., 2004), the same values of $M = 3500$ kg/mol and $\bar{v} = 0.733$ cm^3/g were used for all three proteins. Mean values and standard deviations result from averaging the data for individual models.

*For calculating these values, the consensus models were slightly modified by expressing different weightings of the spheres by different bead radii. The values for V and R_G of these modified models are identical with the mean values given in Table 1.

†The first line refers to models with beads on lattice points and the second to models with beads on centers of gravity.

‡The cited volumes have been corrected by taking into account the packing density (0.6046) of a hexagonal lattice of spheres by rescaling the bead radii.

§Owing to a considerable overlap of the spheres in these models, the calculated volumes were scaled to the mean values obtained for models with beads on lattice points.

placed either at the centers of the hexagonal lattice cells or at their local centers of gravity as calculated from the mass distribution in each cell. The latter variant yielded templates of a more realistic appearance, however, resulted in considerable amounts of overlapping spheres (see Fig. 2, *C* and *E*), whereas the approach using hexagonal lattice points is devoid of overlapping.

Top and side views of selected SAXS-biased DAMMIN models of *Eudistylia* Chl (*D*) and *Macrobdella* Hb (*F*) are also shown in Fig. 2. These models were created using the SAXS templates (*C* and *E*) with overlapping spheres placed at local centers of gravity. The comparison of the templates with the resulting models suggests that the main structural features of the templates were only moderately altered by the DAMMIN procedure. The most obvious changes concern the reduced mass density in the central region of both models (marked by *black circles*). Similar changes were observed with models that were biased by templates consisting of spheres placed exactly at hexagonal lattice points (data not shown).

Surface rendering of the DAMMIN models shown in Fig. 2 visualizes the effects of the applied procedure even more impressively. Though the similarity of the rendered SAXS-biased DAMMIN models in Fig. 3 *b* (*A–D*, *Eudistylia* Chl; *E–H*, *Macrobdella* Hb) with the underlying SAXS consensus models (Fig. 3 *a*) is evident, in the center of both HBL complexes less density is assumed by the DAMMIN models, and the subunits appear to be more hollow than in the SAXS consensus models (cf. the *top views* (*A* and *B*; *E* and *F*), and the central slabs (*D* and *H*) in *a* and *b* of Fig. 3). Moreover, the SAXS-biased DAMMIN models fit the experiment much better; their scattering curves (Fig. 4, *A* and *C*, *green circles* with *error bars*) match the observed data in the angular range $h < 1.7$ nm^{-1} perfectly, whereas the fit by the initial SAXS models (*green lines*) is less satisfactory. The fit of the experimental $p(r)$ functions is nearly perfect (Fig. 4, *B* and *D*). The model parameters, as shown in Table 2, are also in agreement with the observations.

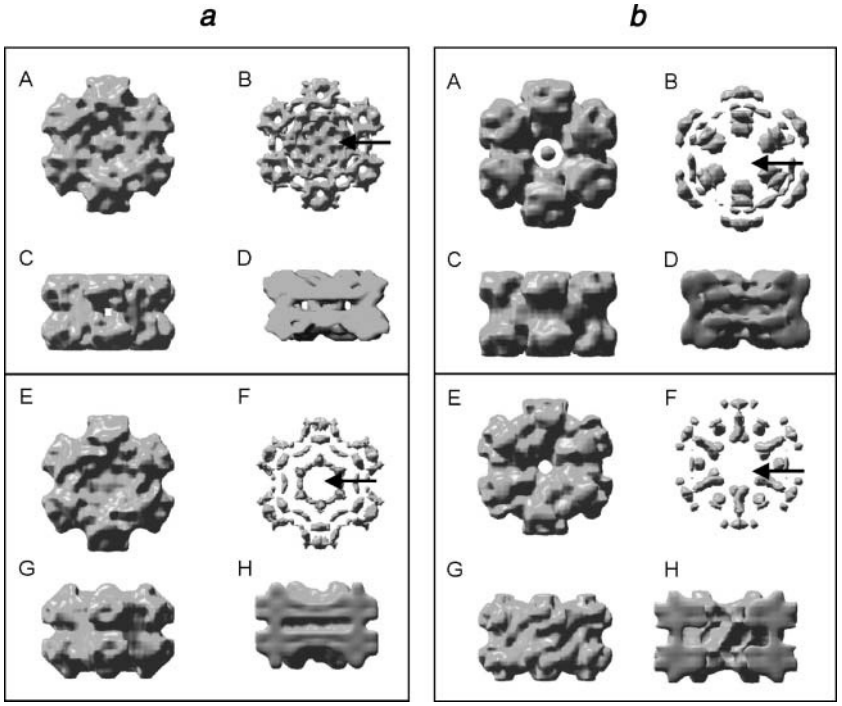

FIGURE 3 Surface representations of the SAXS consensus models (*a*) and SAXS-biased DAMMIN models (*b*) of *Eudistylia* Chl (*A–D*) and *Macrobdella* Hb (*E–H*). The models are shown in top views for two different threshold levels (*A* and *B*; *E* and *F*) to enable a better comparison with other models discussed in the text. The corresponding side views of *A* and *E* are shown in *C* and *G*; cuts through the models (along their *z* axis and just through the subunits) reveal the inner architecture (*D* and *H*). All models appear to have little density in the central unit (see *arrows*), particularly expressed in the models of *Macrobdella* Hb (*F*). The subunits of the bilayer also seem to be slightly hollow, which is more obvious in *Eudistylia* Chl (*D*). Both effects appear to be enhanced in the corresponding SAXS-biased DAMMIN models (*b*).

Ab initio DAMMIN models

DAMMIN models were also created without using templates, to check the influence of these constraints. By this approach, the low-resolution shape and internal structure of the hemoglobins were restored ab initio, exploiting the experimental SAXS curves without any a priori information or with no constraint other than the assumption of D6 symmetry. In accordance with previous observations, only the latter variant resulted in models of physical relevance (Zipper and Durchschlag, 2003; Zipper at al., 2004). Nevertheless, many of the models generated this way represented unrealistic structures and were therefore discarded, although in all cases the experimental scattering curve was fitted perfectly. Models were considered as unrealistic if their appearance deviated substantially from that suggested by EM, e.g., because of the occurrence of central protuberances, isolated spheres, or sphere-like overall shapes. Some typical examples of discarded models are outlined in Fig. 5, to illustrate the philosophy of the applied selection criteria.

Models that had an appearance similar to EM models (de Haas et al., 1996a,b) were chosen for a more detailed analysis. For *Eudistylia* Chl and *Macrobdella* Hb, 11 different ab initio DAMMIN models were used to create averaged ab initio models, similar to the creation of the consensus SAXS models shown in Fig. 2, *A* and *B*. To accumulate structural information that is represented more often in the models, spheres that were not present in at least from two to five models were omitted in the averaging process. All other spheres were weighted according to their frequency of occupancy.

Various averaged ab initio DAMMIN models of *Eudistylia* Chl and *Macrobdella* Hb and their structural and hydrodynamic parameters have been presented elsewhere (Zipper et al., 2004). In this article, we analyze the corresponding surface representations (Fig. 6 *a*). In agreement with the SAXS consensus and SAXS-biased DAMMIN models (Fig. 3), the representations of the averaged ab initio DAMMIN models also show little density in the central unit (Fig. 6 *a*, *arrows*), but unlike the aforementioned models they give, at first sight, no hint for cavities in the 12 subunits. A careful analysis, however, reveals that this is mainly caused by the special process of averaging: most of the ab initio models selected for averaging actually possess small holes in their subunits, but the positions of these holes are quite different in the various models; therefore the averaging procedure results in a blurred density distribution without pronounced minima in the subunits. Owing to the averaging procedure, the distance distribution functions $p(r)$ of the averaged models (Fig. 4, *B* and *D*, *red lines*) differ significantly from the $p(r)$ functions of the original models (*red circles* with *error bars*) that simulate the experimental $p(r)$ functions (*black lines*) almost perfectly. Therefore the averaging procedure also deteriorates the fit of the scattering curves: the curves of the original ab initio DAMMIN models, which were used for averaging, fit the experimental curves within the limits of error up to $h = 1.7\ \mathrm{nm}^{-1}$ (Fig. 4, *A* and *C*, *red circles* with *error bars* and *black lines*), whereas the

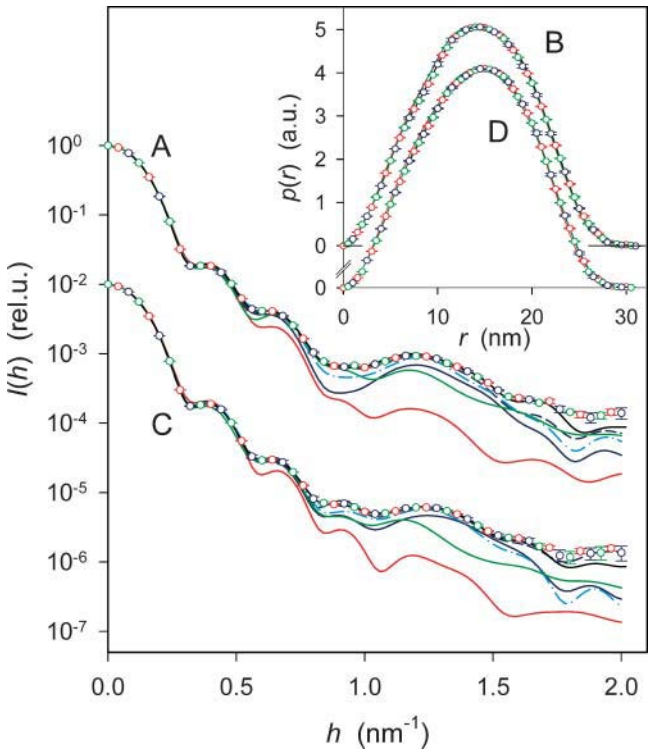

FIGURE 4 Comparison of the experimental scattering curves (*black lines* in *A* and *C*) and pair-distance distribution functions (*black lines* in *B* and *D*) of *Eudistylia* Chl (*A* and *B*) and *Macrobdella* Hb (*C* and *D*) with the scattering curves and $p(r)$ functions of various models. (*Green lines*) SAXS consensus model (average of six (*Eudistylia* Chl) or four (*Macrobdella* Hb) trial-and-error models; bead radius $r_b = 0.66$ nm) as shown in Fig. 2, *A* and *B*. (*Green circles*) Average of the scattering curves or $p(r)$ functions of three DAMMIN models biased by the SAXS consensus models; (*red circles* with *error bars*) average of the scattering curves or $p(r)$ functions of 11 ab initio DAMMIN models; and (*blue circles*) average of the scattering curves or $p(r)$ functions of 18 DAMMIN models biased by 3D reconstructions from cryo-EM. The other colored lines represent the scattering curves or $p(r)$ functions calculated for averaged structures. (*Red lines*) Average of 11 ab initio DAMMIN models (bead radius $r_b = 0.8$ nm; minimal accepted frequency of occupancy $f_{min} = 2$); surface representations of the averaged structures are shown in Fig. 6 *a*; (*solid blue lines* in *A* and *C*) average of 18 EM-biased DAMMIN models of different types ($r_b = 0.8$ or 0.6 nm; beads arranged on hexagonal lattice points or on local centers of gravity; $f_{min} = 1$), surface representations of the averaged structures are shown in Fig. 6 *b*; (*dot-dashed cyan lines* in *A* and *C*) average of six EM-biased DAMMIN models ($r_b = 0.6$ nm; beads on lattice points; $f_{min} = 2$); (*dashed blue lines* in *A* and *C*) average of four EM-biased DAMMIN models ($r_b = 0.8$ nm; beads on local centers of gravity; $f_{min} = 1$). Models representing averaged structures reflect structural tendencies rather than details. Therefore the scattering curves of the averaged DAMMIN models (*blue* and *red lines*) do not fit the experimental data as well as the scattering curves of the individual models (*blue* and *red circles* with *error bars*). The $p(r)$ functions of the averaged EM-biased models agree with the experimental values quite well over the whole range of data, and therefore they are not indicated in *B* and *D*.

curves that were calculated from the averaged structures (*red lines*) deviate remarkably.

EM-biased DAMMIN models

For comparison, we include DAMMIN models that were created making direct use of the precise structural information available from 3D EM reconstructions. The EM density data of *Eudistylia* Chl and *Macrobdella* Hb were provided by F. de Haas and J.-C. Taveau (Laboratoire de Biochimie Fondamentale, University François Rabelais, Tour, France) (for details of the reconstructions, see de Haas et al., 1996a,b). A total of 18 EM-biased models were calculated for each protein, all of them fitting the experimental data very well (*blue circles* with *error bars* in Fig. 4), and the averaged structures are given in Fig. 6 *b* in surface representation (the original models can be found in Zipper et al., 2004). These models clearly show hollow subunits, similar to the original EM reconstructions (de Haas et al., 1996a,b), even after averaging. This demonstrates that DAMMIN neither fills the holes given by the templates nor does it shift their position (which would lead to a blurred electron density distribution, similar to the situation observed for the averaged ab initio models shown in Fig. 6 *a*). In addition, the subunits in the EM-biased DAMMIN models seem to be more hollow than assumed by the SAXS and SAXS-biased models. The density in the central unit appears to be comparable with the SAXS-biased DAMMIN models.

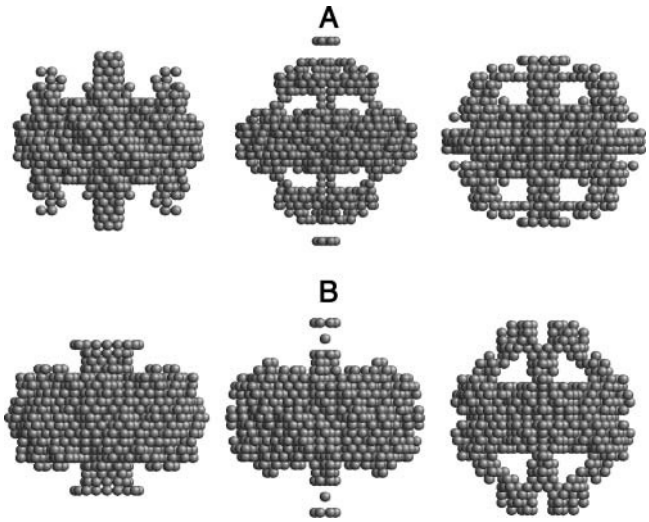

FIGURE 5 Side views of selected ab initio DAMMIN models of *Eudistylia* Chl (*A*) and *Macrobdella* Hb (*B*) that were considered to represent unrealistic structures and were therefore discarded and not used for averaging.

Mass fraction in the central region

All models presented above exhibit a low-density area in the center. To establish a founded basis for a quantitative comparison, the fraction of mass contained in the central region of each individual model was derived from the number of spheres whose centers are located within a radial distance of 4.1, 4.9, and 5.7 nm, respectively, from the center of the model. The data obtained for models belonging to the same type (trial-and-error SAXS models; SAXS-biased, ab initio, and two variants of EM-biased DAMMIN models)

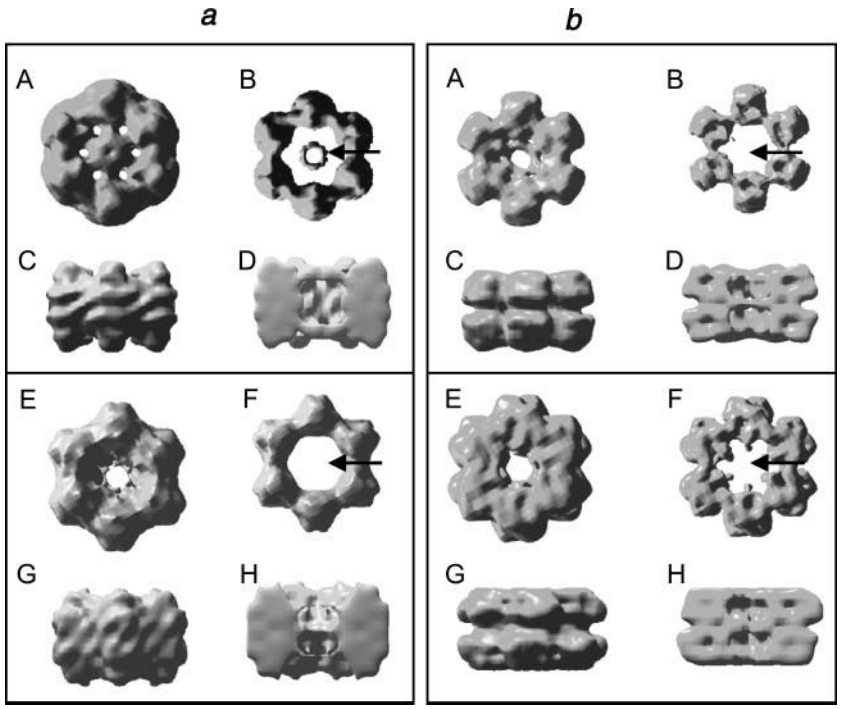

FIGURE 6 Surface representations of averaged ab initio (*a*) and EM-biased (*b*) DAMMIN models of *Eudistylia* Chl (*top*) and *Macrobdella* Hb (*bottom*). The models (with $r_b = 0.8$ nm and (*a*) $f_{min} = 2$ or (*b*) $f_{min} = 1$) are shown in top views for two different threshold levels (*A* and *B*; *E* and *F*), side views of *A* and *E* (*C* and *G*) and cuts along the *z* axis (*D* and *H*). In all four models, very little density is observed in the central unit (*arrows*). The bilayer subunits of the EM-biased models clearly appear to be hollow, in contrast to the subunits of the ab initio models.

were averaged to yield mean mass fractions and the corresponding standard deviations. In the case of models representing averaged structures (SAXS consensus and averaged DAMMIN models), mean mass fractions were also calculated directly from the numbers and statistical weightings of the spheres; if all spheres were taken into account, the same mean values resulted as from the procedure described before, and only slightly different values were obtained if the spheres with the lowest weighting were neglected. To eliminate the trivial effect of the volume, the data shown in Fig. 7 have been normalized to the volume of the sphere with a radius of 4.9 nm; by this normalization procedure, the plotted data become representative of the mean density in the central region. For comparison, the results obtained for *Lumbricus* Hb are included in Fig. 7.

Prediction of hydrodynamic properties

The translational diffusion coefficient D and sedimentation coefficient s of the various DAMMIN models of the annelid hemoglobins under analysis were predicted from the coordinates of the spheres, upscaling the bead radii appropriately to correct the volumes of the models for the packing density of spheres in a hexagonal lattice. Because of the currently available computer facilities, the prediction of the hydrodynamic parameters of the SAXS consensus models was performed for the first time without a preceding data reduction step (cf. Zipper and Durchschlag, 2000; Zipper et al., 2002). This approach was quite challenging considering the large number of beads involved and the inhomogeneous density distributions in the consensus models (for *Lumbricus* Hb, the model presented in Krebs et al., 1998, was used). To take the density distributions adequately into account, the different weightings of the initially equal-sized spheres had to be expressed by different bead volumes. This implied the use of different radii, whereas the coordinates of the spheres were not altered. The results of the hydrodynamic predictions are included in Table 2.

DISCUSSION

Comparison of the different modeling approaches

Important decisive factors for evaluating the goodness of 3D structures restored from low-resolution SAXS data of biopolymers usually include the extent to which the experimental scattering data and derived parameters are simulated by the respective models, the problem of uniqueness, and the physical relevance of the models. Following these criteria, the SAXS consensus models of *Eudistylia* Chl and *Macrobdella* Hb, averaged from selected trial-and-error models and shown in Figs. 2, *A* and *B*, and 3 *a*, are good approximations to the protein solution structure, but they are certainly not perfect: principal structural features of the HBL complexes (overall structure, central unit, and hollow subunits) are presumably met by the models quite well, and the problem of uniqueness has been reduced by the averaging procedure applied, but the experimental $I(h)$ and $p(r)$ patterns are neither fitted satisfactorily by the consensus models (Fig. 4, *green lines*) nor by the underlying trial-and-error approaches (data not shown). Nevertheless, the

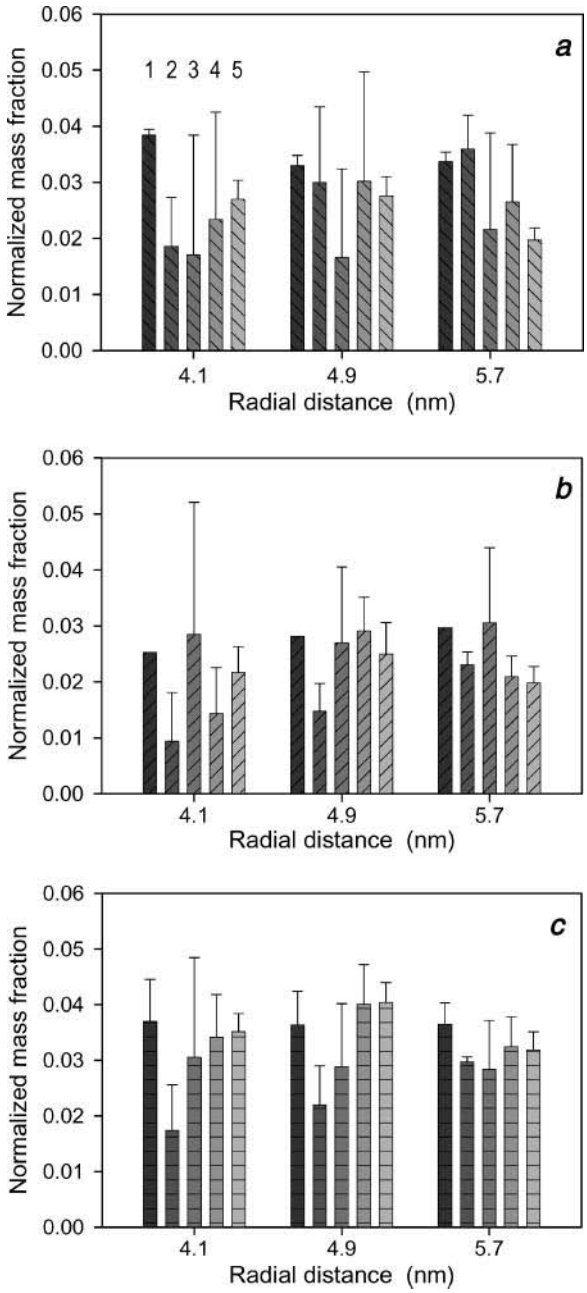

FIGURE 7 The mean fraction of mass in the central region of different models of *Eudistylia* Chl (*a*), *Macrobdella* Hb (*b*), and *Lumbricus* Hb (*c*) as derived from the number of spheres located within a radial distance of 4.1, 4.9, and 5.7 nm from the center, normalized to a constant volume (sphere of 4.9 nm radius) to become representative of the density. The limits of error represent the standard deviation obtained from averaging the data for the respective set of models. From left to right, the bars correspond to the following five types of models: (*1*) SAXS consensus models (the mean values and standard deviations for *Eudistylia* Chl and *Lumbricus* Hb were calculated from the individual models underlying the consensus models; for technical reasons, the mean values for *Macrobdella* Hb could only be obtained directly from the consensus model, by appropriately taking into account the different weighting of the spheres), (*2*) SAXS-biased DAMMIN models, (*3*) ab initio DAMMIN models, (*4*) DAMMIN models biased by EM-templates with spheres on hexagonal lattice points, and (*5*) DAMMIN models biased by EM-templates with spheres on local centers of gravity.

comparison of the consensus models for the two proteins investigated in this study and for *Lumbricus* Hb (Krebs et al., 1998) points at the presence of low-density areas in all complexes and suggests the occurrence of structural differences.

Areas of low density in protein complexes are often of biological and structural interest. Therefore we paid special attention to their modeling, although this process proved to be quite demanding. DAMMIN analyses of the experimental scattering curves, using templates based on the SAXS consensus models, improved these models considerably. Although the SAXS-biased DAMMIN models essentially retain the gross-structural features of the consensus models (Fig. 3), slight deviations from the original structure occur both in the central unit and the 12 subunits. These changes appear to be responsible for the significantly improved fit to the experimental data (Fig. 4, *green circles* with *error bars*). The results concerning the low-density areas in these DAMMIN models are remarkable because the templates used to generate the models were based on all of the spheres of the respective consensus model but did not contain any information about the different weightings of these spheres.

DAMMIN analyses performed without the usage of templates were challenging because of the problem of uniqueness. The creation of DAMMIN models without any a priori information led to generally unrealistic models (irregular globular shapes and peripheral cavities). The restriction of the DAMMIN procedure to models with D6 symmetry, without using templates, turned out to be a major improvement and led to a variety of models (see Zipper et al., 2004). About 50% of these ab initio models looked quite realistic and were selected for a further analysis; unrealistic models (Fig. 5) were discarded. However, the diversity of the selected structures did not allow choosing a unique model. Therefore an averaging procedure was applied, similar to the creation of the SAXS consensus models. Model averaging is a legitimate procedure to accumulate overall information and to cope with the problem of uniqueness as recently addressed by Volkov and Svergun (2003). The observed loss of information concerning the existence of holes in the subunits as a consequence of averaging indicates that the DAMMIN procedure, though being capable of detecting ab initio inhomogeneities in the density distribution of the complexes, has difficulties in locating them with a sufficient degree of reliability because of the limited resolution of the SAXS experiments and the usage of three-dimensionally averaged information from specimens in solution.

Obviously, SAXS alone cannot precisely locate low-density areas in these protein complexes, and structural information on a high-resolution level cannot be expected. Therefore, an improvement was attempted by DAMMIN analyses importing a priori structural information from 3D EM reconstructions through appropriate templates. This tactic turned out to be a highly promising way, by combining structural data from different methods and at unequal levels of resolution. The resulting EM-biased DAMMIN models

are of higher quality and relevance for the solution structure than the models originating merely from SAXS studies and fit the experimental SAXS data much better than EM-based models that were established without the application of the DAMMIN program as in a previous study on *Lumbricus* Hb (Krebs et al., 1998).

The central unit

The high similarity of the experimental SAXS data of *Eudistylia* Chl and *Macrobdella* Hb (Fig. 1) suggests that their solution structures can only differ slightly. From our trial-and-error and consensus SAXS models, we conclude that major structural differences occur in the central region of the complexes. According to our data (Table 1, number of high-weight spheres in the central unit), *Macrobdella* Hb has a very small central unit, whereas the central mass of *Eudistylia* Chl seems to be more similar to that of *Lumbricus* Hb. The mean values of the mass fractions in the central region of the SAXS models and the SAXS-biased DAMMIN models up to the chosen radii are in full accord with these findings; the normalized mass fractions presented in Fig. 7 reflect the differences between the models impressively and allow a direct comparison of the mean densities in the central region. A smaller central mass in *Macrobdella* Hb also follows from the mass fractions obtained from the EM-biased models. All of these results are in good agreement with the observed differences in the structure of the central units in 3D EM reconstructions (de Haas et al., 1996a,b). The finding that the analyzed ab initio DAMMIN models yield mass fractions for *Macrobdella* Hb that are closer to the values for *Lumbricus* Hb than for *Eudistylia* Chl is less important in view of the large standard deviations of these results, corroborating the problem of uniqueness.

A very small and subtle central subunit was first described by Ohtsuki and Crewe (1983), after the results of earlier SAXS experiments (Pilz et al., 1980) that already postulated a central subunit in the center of *Lumbricus* Hb. The first EM reconstruction of *Lumbricus* Hb reached a resolution of 3 nm (Schatz et al., 1995). In the center of the molecule, a doughnut shape of ~5 nm height and 12 nm diameter was found; it exhibited a central hole ~2.5 nm wide, which was close to the resolution limit achieved in that study. This additional subunit was assumed to accommodate 12 linker chains. From the crystallographic reconstruction to 0.55 nm, we know that indeed only linker chains are present toward the center (Royer et al., 2000). Very unexpected in this context was the finding that 12 triple-stranded coiled-coil helices are present in this area. Thus emanating from each one-twelfth subunit are three 4.5-nm long rods consistent with coiled-coil α-helices. A hole of ~4.5 nm diameter in the center of the molecule and the region where only the triple-stranded linker helices are present constitute a low-density area with ~10–12 nm diameter in the center of *Lumbricus* Hb.

At a resolution of 3.5 nm, EM reconstructions of the Chl from the polychaete *E. vancouverii* show little density (a flat hexagonal mass) in the center (de Haas et al., 1996b). By contrast, the central region of *Macrobdella* Hb contains a hexagonal toroid at a resolution of 4 nm (de Haas et al., 1996a). The structural role of the toroid was assumed to be a pier to which two bracelets are fixed by 12 connections. In the polychaete worm *Arenicola marina*, the central subunit appears as an ellipsoid in EM reconstructions at 2.5 nm (Jouan et al., 2001).

Hollow globular subunits

In EM reconstructions, the subunits themselves are found to be hollow (de Haas et al., 1996a,b). The SAXS consensus models show slight density variations in the subunits but to a much lesser extent than observed in the EM reconstructions. A refinement of the SAXS consensus models by DAMMIN makes their subunits much more hollow (see Fig. 3). Of the ab initio DAMMIN models, which were generated without bias, some assume filled subunits without density variation, whereas others definitely possess holes in their subunits, at positions that are different for each model. Accordingly, averaging the structures of the ab initio models leads to a nearly complete loss of information concerning density variations in the subunits (see Fig. 6 *a*). If internal cavities are part of the structure of a template imported by DAMMIN as a priori structural information, such holes are not filled up but are rather enlarged by DAMMIN. This is the case with the SAXS-biased and, even more expressed, with the EM-biased DAMMIN models (see Figs. 3 *b* and 6 *b*).

Oblate anisometry

Apart from the aforementioned differences in the central units, dissimilarities between *Eudistylia* Chl, *Macrobdella*, and *Lumbricus* Hb are also suggested by their different experimental volumes V, which are reproduced almost perfectly by all modeling approaches applied, and also by a critical analysis of the data obtained for the dimensions of the proteins in the three directions of space (see Tables 1 and 2). The comparison of the values for d_z, the dimension in z direction, gives some hint that the height of *Eudistylia* Chl might be lower than that of the other proteins under investigation; however, the considerable limits of error of some d_z values do not allow a founded decision. Similarly, the comparison of the radii of gyration in the three directions of space, R_x, R_y, and R_z, is not conclusive in most cases because of the too large uncertainties of the quantities to be compared. Only the modeling approach making use of EM-based templates with the beads on local centers of gravity is able to unveil significant differences in the mass distribution of *Eudistylia* Chl and *Macrobdella* or *Lumbricus* Hb. According to the results obtained by this approach, the ratio R_z/R_x of the axial radii of gyration, a measure of the oblate

anisometry, is 0.621 ± 0.003 for *Eudistylia* Chl, 0.648 ± 0.006 for *Macrobdella* Hb, and 0.665 ± 0.005 for *Lumbricus* Hb. The comparison of these values with the corresponding ratios for the used EM templates (*Eudistylia* Chl template, 0.753; *Macrobdella* Hb template, 0.731; and *Lumbricus* Hb template, 0.714) convincingly shows that the ratios given above present real results of the DAMMIN analysis of the experimental scattering curves and are not imported from the templates. Similar differences in the particle dimensions and volume between *Eudistylia* Chl and *Lumbricus* Hb as observed by us were also suggested by EM studies (Qabar et al., 1991).

Hydrodynamic parameters

As follows from Table 2, the parameters D and s predicted for the consensus models of *Eudistylia* Chl and *Macrobdella* Hb are quite similar to the values anticipated for the corresponding *Lumbricus* Hb model. While predicted D values for *Lumbricus* Hb are in the range of the experimental data found in the literature, the values predicted for s exceed the experimental ones slightly (cf. Table 2 legend).

The prediction of D values for the various DAMMIN models led to nearly identical results for the three proteins (Table 2). With each of the different types of DAMMIN models (SAXS-biased, ab initio, and EM-biased) the D values predicted for the three proteins always agree within the limits of error (~1% in most cases). Slightly larger differences can be observed, on the other hand, between the predictions for different types of DAMMIN models. Ab initio models show the lowest D values, whereas EM-biased models, with the beads on centers of gravity, give the highest values; the differences do not exceed, however, a few percent. It must be borne in mind that for the prediction of D values the molar mass M and the partial specific volume $\bar{v}$ of the proteins are not used. For the prediction of s values, on the other hand, both M and $\bar{v}$ are required. Usage of the same M and $\bar{v}$ values for all three proteins leads to very consistent results for s (Table 2). At least for *Macrobdella* Hb, this approach is in good agreement with data reported for M and $\bar{v}$ (Weber et al., 1995). On the other hand, lower s values for *Eudistylia* Chl and *Macrobdella* Hb would be obtained by the usage of our experimentally observed M values (Table 1) for these proteins. In the extreme case of *Eudistylia* Chl, the s values predicted this way would be even lower than the very low experimental value (cf. Table 2). For *Lumbricus* Hb, the predictions for D from the DAMMIN models are in accord with values from the literature, whereas the predicted s values are slightly larger than the observed values.

CONCLUSIONS

In this study, the solution structures of *Eudistylia* Chl and *Macrobdella* Hb were investigated by the SAXS technique, and models were established by different procedures. The following conclusions can be drawn:

1. The creation of SAXS models by trial and error is a time-consuming and tedious procedure to gain structural information. Application of advanced, automated modeling procedures like the one implemented in Svergun's program DAMMIN provides a valuable alternative. The options to define symmetry constraints or to import templates make the program DAMMIN a most powerful tool. Owing to the symmetry options, DAMMIN is clearly superior to other programs that have been tested for their efficiency in analyzing HBL structures (cf. Zipper et al., 2002; Zipper and Durchschlag, 2003).
2. According to our data, the Chl from *E. vancouverii* and the Hbs from *M. decora* and *L. terrestris* appear to be very similar, but they differ in their overall dimensions. Different amounts of density were simulated in the center of the proteins, and for *Macrobdella* Hb the smallest amount of density was simulated in all model approaches.
3. Most interestingly, all modeling approaches simulate an inhomogeneous density distribution within the 12 subunits, meaning that there are areas in the interior of the models that contain less spheres. This is remarkable because the origin and a priori information content of the various models is quite different. Without a priori information, DAMMIN cannot locate these low-density areas with sufficient accuracy but places them in different ab initio models at varying positions. The usage of templates, however, improves the results. Since density variations in protein complexes are of particular interest, their detection is highly desirable. Variations that are small and buried within the protein are hard to detect, but putative information may be gained even in such cases by applying sophisticated SAXS modeling procedures.
4. Averaging of models is a legitimate procedure to point out structural tendencies by emphasizing the most persistent features. In this way, important, reoccurring features in the protein structure can be spotted and interpreted accordingly. Structural details at high resolution, however, may be lost during the averaging procedure, and the averaged model may also provide a worse fit of the experimental data. Despite these reservations, averaging can be a valuable tool to reduce the problem of the uniqueness of shape reconstructions.

The authors are much obliged to S. N. Vinogradov for a gift of the proteins, to F. de Haas and J.-C. Taveau for providing the 3D reconstructions of the annelid hemoglobins analyzed, and to D. I. Svergun, J. García de la Torre, and R. A. Sayle for the use of the programs DAMMIN and GNOM, HYDRO, and RASMOL, respectively.

This work was supported by the Austrian Academy of Sciences (to A.K.) and the Austrian ''Fonds zur Förderung der wissenschaftlichen Forschung'' (to A.K. and P.Z.).

REFERENCES

Boekema, E. J., and M. van Heel. 1989. Molecular shape of *Lumbricus terrestris* erythrocruorin studied by electron microscopy and image analysis. *Biochim. Biophys. Acta.* 957:370–379.

Collaborative Computational Project, Number 4. 1994. The CCP4 suite: programs for protein crystallography. *Acta Cryst.* D50:760–763.

David, M. M., and E. Daniel. 1974. Subunit structure of earthworm erythrocruorin. *J. Mol. Biol.* 87:89–101.

de Haas, F., N. Boisset, J.-C. Taveau, O. Lambert, S. N. Vinogradov, and J. N. Lamy. 1996a. Three-dimensional reconstruction of *Macrobdella decora* (Leech) hemoglobin by cryoelectron microscopy. *Biophys. J.* 70:1973–1984.

de Haas, F., A. Kuchumov, J.-C. Taveau, N. Boisset, S. N. Vinogradov, and J. N. Lamy. 1997. Three-dimensional reconstruction of native and reassembled *Lumbricus terrestris* extracellular hemoglobin. Localization of the monomeric globin chains. *Biochemistry.* 36:7330–7338.

de Haas, F., J.-C. Taveau, N. Boisset, O. Lambert, S. N. Vinogradov, and J. N. Lamy. 1996b. Three-dimensional reconstruction of the chlorocruorin of the polychaete annelid *Eudistylia vancouverii*. *J. Mol. Biol.* 255: 140–153.

García de la Torre, J., M. L. Huertas, and B. Carrasco. 2000. Calculation of hydrodynamic properties of globular proteins from their atomic-level structure. *Biophys. J.* 78:719–730.

García de la Torre, J., S. Navarro, M. C. López Martínez, F. G. Díaz, and J. J. López Cascales. 1994. HYDRO: a computer program for the prediction of hydrodynamic properties of macromolecules. *Biophys. J.* 67:530–531.

Glatter, O. 1977. A new method for the evaluation of small-angle scattering data. *J. Appl. Crystallogr.* 10:415–421.

Glatter, O. 1980. Computation of distance distribution functions and scattering functions of models for small angle scattering experiments. *Acta Phys. Austriaca.* 52:243–256.

Glatter, O., and O. Kratky, editors.1982. Small Angle X-ray Scattering. Academic Press, London, UK.

Gros, G. 1978. Concentration dependence of the self-diffusion of human and *Lumbricus terrestris* hemoglobin. *Biophys. J.* 22:453–468.

Jouan, L., J.-C. Taveau, S. Marco, F. H. Lallier, and J. N. Lamy. 2001. Occurrence of two architectural types of hexagonal bilayer hemoglobin in annelids: comparison of 3D reconstruction volumes of *Arenicola marina* and *Lumbricus terrestris* hemoglobins. *J. Mol. Biol.* 305:757–771.

Kapp, O. H., A. N. Qabar, M. C. Bonner, M. S. Stern, D. A. Walz, M. Schmuck, I. Pilz, J. S. Wall, and S. N. Vinogradov. 1990. Quaternary structure of the giant extracellular hemoglobin of the leech *Macrobdella decora*. *J. Mol. Biol.* 213:141–158.

Krebs, A. 1996. Röntgenkleinwinkelstreuung an extrazellulären Sauerstofftransportproteinen und an einer Phosphorylase. PhD thesis. University of Graz, Austria.

Krebs, A., J. Lamy, S. N. Vinogradov, and P. Zipper. 1998. *Lumbricus terrestris* hemoglobin: a comparison of small-angle X-ray scattering and cryoelectron microscopy data. *Biopolymers.* 45:289–298.

Krebs, A., P. Zipper, and S. N. Vinogradov. 1996. Lack of size and shape alteration of oxygenated and deoxygenated *Lumbricus terrestris* hemoglobin? *Biochim. Biophys. Acta.* 1297:115–118.

Lamy, J. N., B. N. Green, A. Toulmond, J. S. Wall, R. E. Weber, and S. N. Vinogradov. 1996. Giant hexagonal bilayer hemoglobins. *Chem. Rev.* 96:3113–3124.

Martin, P. D., K. L. Eisele, M. A. Doyle, A. R. Kuchumov, D. A. Walz, E. G. Arutyunyan, S. N. Vinogradov, and B. F. P. Edwards. 1996a. Molecular symmetry of the dodecamer subunit of *Lumbricus terrestris* hemoglobin. *J. Mol. Biol.* 255:170–175.

Martin, P. D., A. R. Kuchumov, B. N. Green, R. W. A. Oliver, E. H. Braswell, J. S. Wall, and S. N. Vinogradov. 1996b. Mass spectrometric composition and molecular mass of *Lumbricus terrestris* hemoglobin: a refined model of its quaternary structure. *J. Mol. Biol.* 255:154–169.

Mouche, F., N. Boisset, and P. A. Penczek. 2001. *Lumbricus terrestris* hemoglobin—the architecture of linker chains and structural variation of the central toroid. *J. Struct. Biol.* 133:176–192.

Ohtsuki, M., and A. V. Crewe. 1983. Evidence for a central substructure in a *Lumbricus terrestris* hemoglobin obtained with STEM low-dose and digital processing techniques. *J. Ultrastruct. Res.* 83:312–318.

Ownby, D. W., H. Zhu, K. Schneider, R. C. Beavis, B. T. Chait, and A. F. Riggs. 1993. The extracellular hemoglobin of the earthworm, *Lumbricus terrestris*. Determination of subunit stoichiometry. *J. Biol. Chem.* 268:13539–13547.

Pilz, I., E. Schwarz, and S. N. Vinogradov. 1980. Small-angle X-ray studies of *Lumbricus terrestris* haemoglobin. *Int. J. Biol. Macromol.* 2:279–283.

Qabar, A. N., M. S. Stern, D. A. Walz, J.-T. Chiu, R. Timkovich, J. S. Wall, O. H. Kapp, and S. N. Vinogradov. 1991. Hierarchy of globin complexes. The quaternary structure of the extracellular chlorocruorin of *Eudistylia vancouverii*. *J. Mol. Biol.* 222:1109–1129.

Rossi Fanelli, M. R., E. Chiancone, P. Vecchini, and E. Antonini. 1970. Studies on erythrocruorin. I. Physicochemical properties of earthworm erythrocruorin. *Arch. Biochem. Biophys.* 141:278–283.

Royer, W. E., Jr., and W. A. Hendrickson. 1988. Molecular symmetry of *Lumbricus* erythrocruorin. *J. Biol. Chem.* 263:13762–13765.

Royer, W. E., Jr., K. Strand, M. van Heel, and W. A. Hendrickson. 2000. Structural hierarchy in erythrocruorin, the giant respiratory assemblage of annelids. *Proc. Natl. Acad. Sci. USA.* 97:7107–7111.

Sayle, R. A., and E. J. Milner-White. 1995. RASMOL: biomolecular graphics for all. *Trends Biochem. Sci.* 20:374–376.

Schatz, M., E. V. Orlova, P. Dube, J. Jäger, and M. van Heel. 1995. Structure of *Lumbricus terrestris* hemoglobin at 30 Å resolution determined using angular reconstitution. *J. Struct. Biol.* 114:28–40.

Schmuck, M. 1989. Röntgenkleinwinkeluntersuchungen an extrazellulären Annelid-hämoglobinen und einer Cellobiohydrolase. PhD thesis. University of Graz, Austria.

Semenyuk, A. V., and D. I. Svergun. 1991. GNOM—a program package for small-angle scattering data processing. *J. Appl. Crystallogr.* 24:537–540.

Shlom, J. M., and S. N. Vinogradov. 1973. A study of the subunit structure of the extracellular hemoglobin of *Lumbricus terrestris*. *J. Biol. Chem.* 248:7904–7912.

Svedberg, T. 1937. The ultra-centrifuge and the study of high-molecular compounds. *Nature.* 139:1051–1062.

Svedberg, T., and I.-B. Eriksson. 1933. The molecular weight of erythrocruorin. *J. Am. Chem. Soc.* 55:2834–2841.

Svergun, D. I. 1999. Restoring low resolution structure of biological macromolecules from solution scattering using simulated annealing. *Biophys. J.* 76:2879–2886.

Svergun, D. I. 2000. Advanced solution scattering data analysis methods and their applications. *J. Appl. Crystallogr.* 33:530–534.

Taveau, J.-C., N. Boisset, S. N. Vinogradov, and J. N. Lamy. 1999. Three-dimensional reconstruction of *Lumbricus terrestris* hemoglobin at 22 Å resolution: intramolecular localization of the globin and linker chains. *J. Mol. Biol.* 289:1343–1359.

Terwilliger, R. C., R. L. Garlick, N. B. Terwilliger, and D. P. Blair. 1975. Molecular weight of *Eudistylia vancouveri* chlorocruorin and its subunits. *Biochim. Biophys. Acta.* 400:302–309.

Vinogradov, S. N., O. H. Kapp, and M. Ohtsuki. 1982. The extracellular haemoglobins and chorocruorins of annelids. In Electron Microscopy of Proteins, Vol. 3. J. R. Harris, editor. Academic Press, London, UK. 135–164.

Vinogradov, S. N., S. D. Lugo, M. G. Mainwaring, O. H. Kapp, and A. V. Crewe. 1986. Bracelet protein: a quaternary structure proposed for the giant extracellular hemoglobin of *Lumbricus terrestris*. *Proc. Natl. Acad. Sci. USA.* 83:8034–8038.

Vinogradov, S. N., and P. K. Sharma. 1994. Preparation and characterization of invertebrate globin complexes. *Methods Enzymol.* 231:112–124.

Vinogradov, S. N., P. K. Sharma, A. N. Qabar, J. S. Wall, J. A. Westrick, J. H. Simmons, and S. J. Gill. 1991. A dodecamer of globin chains is the principal functional subunit of the extracellular hemoglobin of *Lumbricus terrestris*. *J. Biol. Chem.* 266:13091–13096.

Volkov, V. V., and D. I. Svergun. 2003. Uniqueness of ab initio shape determination in small-angle scattering. *J. Appl. Crystallogr.* 36:860–864.

Weber, R. E., H. Malte, E. H. Braswell, R. W. A. Oliver, B. N. Green, P. K. Sharma, A. Kuchumov, and S. N. Vinogradov. 1995. Mass spectrometric composition, molecular mass and oxygen binding of *Macrobdella decora* hemoglobin and its tetramer and monomer subunits. *J. Mol. Biol.* 251:703–720.

Weber, R. E., and S. N. Vinogradov. 2001. Nonvertebrate hemoglobins: functions and molecular adaptations. *Physiol. Rev.* 81:569–628.

Zhu, H., D. W. Ownby, C. K. Riggs, N. J. Nolasco, J. K. Stoops, and A. F. Riggs. 1996. Assembly of the gigantic hemoglobin of the earthworm *Lumbricus terrestris*. *J. Biol. Chem.* 271:30007–30021.

Zipper, P., and H. Durchschlag. 2000. Prediction of hydrodynamic and small-angle scattering parameters from crystal and electron microscopic structures. *J. Appl. Crystallogr.* 33:788–792.

Zipper, P., and H. Durchschlag. 2003. Modeling of protein solution structures. *J. Appl. Crystallogr.* 36:509–514.

Zipper, P., A. Krebs, and H. Durchschlag. 2002. Prediction of hydrodynamic parameters of *Lumbricus terrestris* hemoglobin from small-angle X-ray and electron microscopic structures. *Prog. Colloid Polym. Sci.* 119:141–148.

Zipper, P., A. Krebs, and H. Durchschlag. 2004. Comparative modeling of giant annelid hemoglobins. *Prog. Colloid Polym. Sci.* In press.